REPORT DOCUMENTATION PAGE	Form Approved OMB NO. 0704-0188

The public reporting burden for this collection of information is estimated to average 1 hour per response, including the time for reviewing instructions, searching existing data sources, gathering and maintaining the data needed, and completing and reviewing the collection of information. Send comments regarding this burden estimate or any other aspect of this collection of information, including suggesstions for reducing this burden, to Washington Headquarters Services, Directorate for Information Operations and Reports, 1215 Jefferson Davis Highway, Suite 1204, Arlington VA, 22202-4302. Respondents should be aware that notwithstanding any other provision of law, no person shall be subject to any oenalty for failing to comply with a collection of information if it does not display a currently valid OMB control number.
PLEASE DO NOT RETURN YOUR FORM TO THE ABOVE ADDRESS.

1. REPORT DATE (DD-MM-YYYY) 01-07-2016	2. REPORT TYPE Final Report	3. DATES COVERED (From - To) 1-Oct-2009 - 30-Sep-2015

4. TITLE AND SUBTITLE Final Report: WHITEPAPER; Research Area 8; Control of cellular structural networks through unstructured protein domains	5a. CONTRACT NUMBER W911NF-09-1-0507
	5b. GRANT NUMBER
	5c. PROGRAM ELEMENT NUMBER 611103
6. AUTHORS Sanjay Kumar	5d. PROJECT NUMBER
	5e. TASK NUMBER
	5f. WORK UNIT NUMBER

7. PERFORMING ORGANIZATION NAMES AND ADDRESSES University of California - Berkeley Sponsored Projects Office 2150 Shattuck Avenue, Suite 300 Berkeley, CA 94704 -5940	8. PERFORMING ORGANIZATION REPORT NUMBER

9. SPONSORING/MONITORING AGENCY NAME(S) AND ADDRESS (ES) U.S. Army Research Office P.O. Box 12211 Research Triangle Park, NC 27709-2211	10. SPONSOR/MONITOR'S ACRONYM(S) ARO
	11. SPONSOR/MONITOR'S REPORT NUMBER(S) 54705-LS-PCS.12

12. DISTRIBUTION AVAILIBILITY STATEMENT

Approved for Public Release; Distribution Unlimited

13. SUPPLEMENTARY NOTES
The views, opinions and/or findings contained in this report are those of the author(s) and should not contrued as an official Department of the Army position, policy or decision, unless so designated by other documentation.

14. ABSTRACT
The goal of this project is to implement a research program in cellular bioengineering that focuses on hierarchical structural and mechanical networks in cells. The research plan seeks to determine the role of molecular-scale steric forces on the assembly, mechanics, and cell structural contributions of UPDs. There are three aims: (1) To determine the quantitative relationship between chain phosphorylation and steric repulsive properties of UPDs in vitro; (2) To experimentally test the hypothesis that altering neurofilament UPD phosphorylation alters morphology, mechanics, and neurogenesis in neural stem cells; (3) To develop and use multiscale computational

15. SUBJECT TERMS
smart materials, disordered proteins, neurofilaments

16. SECURITY CLASSIFICATION OF:			17. LIMITATION OF ABSTRACT	15. NUMBER OF PAGES	19a. NAME OF RESPONSIBLE PERSON Sanjay Kumar
a. REPORT UU	b. ABSTRACT UU	c. THIS PAGE UU	UU		19b. TELEPHONE NUMBER 510-643-0787

Standard Form 298 (Rev 8/98)
Prescribed by ANSI Std. Z39.18

Report Title

Final Report: WHITEPAPER; Research Area 8; Control of cellular structural networks through unstructured protein domains

ABSTRACT

The goal of this project is to implement a research program in cellular bioengineering that focuses on hierarchical structural and mechanical networks in cells. The research plan seeks to determine the role of molecular-scale steric forces on the assembly, mechanics, and cell structural contributions of UPDs. There are three aims: (1) To determine the quantitative relationship between chain phosphorylation and steric repulsive properties of UPDs in vitro; (2) To experimentally test the hypothesis that altering neurofilament UPD phosphorylation alters morphology, mechanics, and neurogenesis in neural stem cells; (3) To develop and use multiscale computational modeling approaches to relate cytoskeletal protein phosphorylation to cellular mechanical properties.

Enter List of papers submitted or published that acknowledge ARO support from the start of the project to the date of this printing. List the papers, including journal references, in the following categories:

(a) Papers published in peer-reviewed journals (N/A for none)

<u>Received</u>   <u>Paper</u>

07/27/2012 4.00 Nithya Srinivasan, Sanjay Kumar. Ordered and disordered proteins as nanomaterial building blocks,
Wiley Interdisciplinary Reviews: Nanomedicine and Nanobiotechnology, (03 2012): 0. doi: 10.1002/wnan.1160

07/27/2012 5.00 Albert J. Keung, Elena M. de Juan-Pardo, David V. Schaffer, Sanjay Kumar. Rho GTPases Mediate the Mechanosensitive Lineage Commitment of Neural Stem Cells,
STEM CELLS, (11 2011): 1886. doi: 10.1002/stem.746

08/10/2011 1.00 Amit Pathak, Sanjay Kumar. Biophysical regulation of tumor cell invasion: moving beyond matrix stiffness,
Integrative Biology, (01 2011): 267. doi: 10.1039/c0ib00095g

08/10/2011 2.00 Amit Pathak, Sanjay Kumar. From Molecular Signal Activation to Locomotion: An Integrated, Multiscale Analysis of Cell Motility on Defined Matrices,
PLoS ONE, (3 2011): 18423. doi: 10.1371/journal.pone.0018423

08/10/2011 3.00 Shamik Sen, Win Pin Ng, Sanjay Kumar. Contractility Dominates Adhesive Ligand Density in Regulating Cellular De-adhesion and Retraction Kinetics,
Annals of Biomedical Engineering, (10 2010): 1163. doi: 10.1007/s10439-010-0195-z

08/13/2013 7.00 Albert J. Keung, Meimei Dong, David V. Schaffer, Sanjay Kumar. Pan-neuronal maturation but not neuronal subtype differentiation of adult neural stem cells is mechanosensitive,
Scientific Reports, (05 2013): 0. doi: 10.1038/srep01817

TOTAL: **6**

Number of Papers published in peer-reviewed journals:

(b) Papers published in non-peer-reviewed journals (N/A for none)

<u>Received</u>   <u>Paper</u>

TOTAL:

Number of Papers published in non peer-reviewed journals:

(c) Presentations

Number of Presentations: 0.00

Non Peer-Reviewed Conference Proceeding publications (other than abstracts):

<u>Received</u>   <u>Paper</u>

TOTAL:

Number of Non Peer-Reviewed Conference Proceeding publications (other than abstracts):

Peer-Reviewed Conference Proceeding publications (other than abstracts):

<u>Received</u>   <u>Paper</u>

TOTAL:

Number of Peer-Reviewed Conference Proceeding publications (other than abstracts):

(d) Manuscripts

<u>Received</u>   <u>Paper</u>

TOTAL:

Number of Manuscripts:

Books

<u>Received</u>   <u>Book</u>

TOTAL:

<u>Received</u>   <u>Book Chapter</u>

TOTAL:

Patents Submitted

INTRINSICALLY DISORDERED PROTEIN BRUSHES

Patents Awarded

Awards

Elected Fellow, American Institute for Medical and Biological Engineering

Graduate Students

NAME	PERCENT_SUPPORTED	Discipline
Jessica Lee	1.00	
FTE Equivalent:	**1.00**	
Total Number:	**1**	

Names of Post Doctorates

NAME	PERCENT_SUPPORTED
Badriprasad Ananthanarayanan	0.46
Maniraj Bhagawati	1.00
Nithya Srinivasan	0.96
FTE Equivalent:	**2.42**
Total Number:	**3**

Names of Faculty Supported

NAME	PERCENT_SUPPORTED	National Academy Member
Sanjay Kumar	0.11	
FTE Equivalent:	**0.11**	
Total Number:	**1**	

Names of Under Graduate students supported

NAME	PERCENT_SUPPORTED	Discipline
Chiao-Chun Yang	0.01	
Augusta Broughton	0.01	
FTE Equivalent:	**0.02**	
Total Number:	**2**	

Student Metrics
This section only applies to graduating undergraduates supported by this agreement in this reporting period

The number of undergraduates funded by this agreement who graduated during this period: 2.00

The number of undergraduates funded by this agreement who graduated during this period with a degree in science, mathematics, engineering, or technology fields:----- 2.00

The number of undergraduates funded by your agreement who graduated during this period and will continue to pursue a graduate or Ph.D. degree in science, mathematics, engineering, or technology fields:----- 2.00

Number of graduating undergraduates who achieved a 3.5 GPA to 4.0 (4.0 max scale):...... 2.00

Number of graduating undergraduates funded by a DoD funded Center of Excellence grant for Education, Research and Engineering:...... 0.00

The number of undergraduates funded by your agreement who graduated during this period and intend to work for the Department of Defense 0.00

The number of undergraduates funded by your agreement who graduated during this period and will receive scholarships or fellowships for further studies in science, mathematics, engineering or technology fields: 0.00

Names of Personnel receiving masters degrees

NAME
Total Number:

Names of personnel receiving PHDs

NAME
Jessica Lee
Total Number: **1**

Names of other research staff

NAME   PERCENT_SUPPORTED

FTE Equivalent:
Total Number:

Sub Contractors (DD882)

Inventions (DD882)

5   **INTRINSICALLY DISORDERED PROTEIN BRUSHES**

Patent Filed in US? (5d-1) Y

Patent Filed in Foreign Countries? (5d-2)   N

Was the assignment forwarded to the contracting officer? (5e) N
Foreign Countries of application (5g-2):

5a: Badriprasad Ananthanarayanan

5f-1a: University of California, Berkeley

5f-c: 1304 Dartmouth St.

Albany   CA   94706

5a: Maniraj Bhagawati

5f-1a: University of California, Berkeley

5f-c: 101 Crosby CT. #1

Walnut Creek   CA   94598

5a: Sanjay Kumar

5f-1a: University of California, Berkeley

5f-c: 39 Lenelle Ct.

Moraga   CA   94556

5a: Nithya Srinivasan

5f-1a: University of California, Berkeley

5f-c: 265 Camelback Road Apt 106

Pleasant Hill   CA   94523

Scientific Progress

Please see attachment.

Technology Transfer

None to report

FINAL REPORT

Control of cellular structural networks through unstructured protein domains
ARO PECASE W911NF0910507 (10/01/2009 – 09/30/2015)
PI: Sanjay Kumar, M.D., Ph.D.
University of California, Berkeley

The goal of this project has been to implement a research program in cellular bioengineering that focuses on hierarchical structural and mechanical networks in cells. The research plan seeks to determine the role of molecular-scale steric forces on the assembly, mechanics, and cell structural contributions of intrinsically disordered proteins (IDPs). There were three aims: (1) To determine the quantitative relationship between chain phosphorylation and steric repulsive properties of IDPs in vitro; (2) To experimentally test the hypothesis that altering neurofilament IDP phosphorylation alters morphology, mechanics, and neurogenesis in neural stem cells; (3) To develop and use multiscale computational modeling approaches to relate cytoskeletal protein phosphorylation to cellular mechanical properties.

This **final progress report** covers the entire grant period, which includes the original five-year award period (8/01/2009 – 07/31/2014) plus a one-year no-cost extension (08/01/2014 - 07/31/2015).

<u>Overview.</u> An important goal of this program is to characterize the quantitative relationship between the phosphorylation state of NF sidearm domains and the repulsive force generated by the sidearm brush. As described in previous reports, we took a two-pronged approach that involves synthesis and characterization of engineered oligopeptides and full-length proteins that mimic the NF-H sidearm domain. In both cases, our goal has been to characterize molecular conformational properties as a function of sequence and charge state both in solution and when these molecules are tethered to surfaces as an oriented monolayer.

A. PEPTIDE-BASED STRATEGY
As described in previous progress reports, we have submitted and won competitive user proposals to the DOE-supported Molecular Foundry at Lawrence Berkeley National Laboratory (adjacent to the UC Berkeley campus) to synthesize, purify, and characterize NF-mimetic peptides featuring varying numbers of KSP-based repeats found in the human NF protein. For the past year, we have focused on the assembly and characterization of a four-repeat peptide in two variants: one in which all *none* of the serines are mutated ("KSP peptide"), and one peptide in *all* of the serines are mutated to aspartate (D) to mimic phosphorylation ("KDP peptide").

KSP peptide: CEA**KSP**VKEEA**KSP**AEA**KSP**EKEEA**KSP**AEVK [net charge -1 at pH 7]
KDP peptide: CEA**KDP**VKEEA**KDP**AEA**KDP**EKEEA**KDP**AEVK [net charge -5 at pH 7]

Conformational dynamics of peptides in solution
We first characterized the conformational properties of each peptide in solution using small angle X-ray scattering (SAXS), which has been extensively applied to capture solution dimensions of both structured and disordered proteins and peptides.[4-6] Kratky plots of the SAXS data for the two peptides in HEPES buffered saline (HBS, ionic strength 150 mM, pH 7.5) reveal a plateau at high value of the scattering vector, q, which is the signature characteristic of random coils (Figure 1B).[4] This confirms that these peptides lack structure, as expected. In order to extract quantitative information on peptide dimensions from the scattering data, we utilized the ensemble-optimized modeling (EOM) method, which has been previously established to be a more potent scheme than the traditional Guinier approach for interpreting SAXS spectra of intrinsically disordered proteins.[7, 8] Modeling the data in this fashion, we obtained radii of gyration (R_g) of 2.01 ± 0.06 nm and 1.88 ± 0.05 nm for the KDP and KSP peptides, respectively.
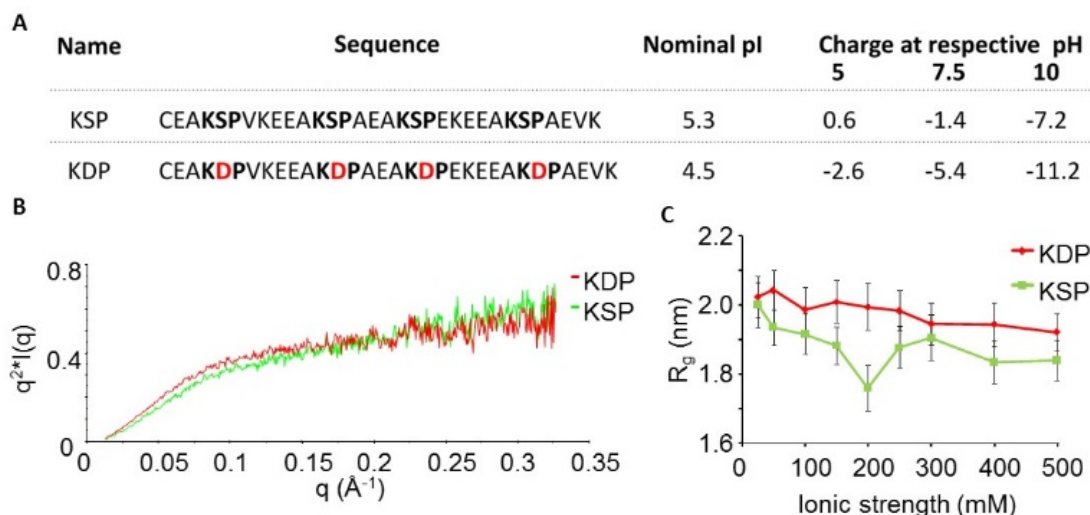
Figure 1 (A) Details of the peptides used in this study. (B) Kratky plots derived from small angle X-ray scattering (SAXS) of the two peptides dissolved in buffer of ionic strength 150 mM, pH 7.5. (C) Radii of gyration (R_g) of the peptides calculated using ensemble optimized modeling of the SAXS spectra of the peptides in buffers of varying ionic strength at pH 7.5. The error bars represent standard deviations of radii of gyration obtained from EOM modeling of datasets from three SAXS measurements at each ionic strength.

The lower R_g of the KSP peptide is consistent with recent molecular dynamics (MD) simulations of the C-terminal tails of the NF-H protein,[9] which found that the non-phosphorylated sidearm domain is stabilized by salt bridges between glutamate and lysine residues; these attractive electrostatic interactions would presumably be destabilized by the electrostatic repulsions associated with added negative charge upon phosphorylation. To investigate these electrostatic effects in a more detailed manner, we next conducted SAXS experiments on the peptides as a function of ionic strength. Interestingly, the dependence of R_g on ionic strength for the KSP and KDP peptides (also calculated using EOM, Figure 1C) exhibit distinct behavior. The R_g of KDP decreases monotonically with ionic strength (correlation coefficient R=-0.94 between R_g and ionic strength). This is consistent with classical polyelectrolyte theory, which would predict that salt-mediated screening of electrostatic repulsions within the peptide should induce chain condensation. The R_g of the KSP peptide, in contrast, initially falls with increasing ionic strength for ionic strength < 200 mM and then rises again for ionic strength > 200 mM. Aspects of these trends are predicted by the polyampholyte theory of Higgs and Joanny,[10] which has been previously used for modeling the R_g of short intrinsically disordered proteins of approximately 50 residues in solutions of guanidium hydrochloride.[11] According to this theory, for polyampholytes with high net charge, the R_g is expected to fall with increasing ionic strength, while for polyampholytes with medium net charge, the R_g is expected to fall up to a critical ionic strength, followed by an increase. These trends are qualitatively in tune with our observations, with the nominal net charge on KSP and KDP being -1 (medium) and -5 (high) (7 positive charges for both, and 8 and 12 negative charges for KSP and KDP respectively). Interestingly, MD simulations of the full-length sidearm domain of NF-H show that the R_g of the phosphorylated sidearm is expected to decrease with increasing ionic strength as we have observed. For the non-phosphorylated sidearm domain, the Rg is expected to remain constant up to an ionic strength of approximately 40 mM, followed by a small increase.[12]

Conformational dynamics of peptide brushes

Having verified the stimulus-responsive properties of these peptides in solution, we next attempted to study their behavior in the form of surface-anchored brushes. This geometry is broadly reminiscent of the *in vivo* arrangement of NF-H sidearm domains within the axon, which project from the NF core to form cylindrical brushes. Moreover, as discussed earlier, the potential technological application of surface-grafted IDPs as biologically encoded interfacial materials makes this a very useful paradigm to study.[13-15] We therefore immobilized KSP and KDP peptides via their N-terminal cysteine residues on gold substrates and followed the grafting kinetics using surface plasmon resonance (SPR) (Figure 2A). We calculated grafting densities of 0.46 molecules/nm^2 and 0.5 molecules/nm^2 for KSP and KDP peptides, respectively. Assuming square (two-dimensional cubic) packing, this corresponds to a nearest-neighbor grafting distance of 1.47 nm for KSP and 1.41 nm for KDP. These distances are smaller than the end-to-end distances for the two peptides (4.61 nm for KSP and 4.92 nm for KDP), which can be calculated from the R_g values measured from SAXS (Figure 1C).

Based on this high surface density, we conclude that the peptides form brushes on the surface. To measure the brush height, we used a SPR-based methodology recently introduced by Schoch et al. in which bovine serum albumin (BSA) is used as a probe to measure the thicknesses of surface-grafted synthetic polymer and protein layers.[16, 17] In this method BSA molecules experience a steric repulsive force from the polymer/protein brush (proportional to the excluded volume of the polymer layers), which hinders their approach to the SPR transducer. The SPR response of the BSA molecules is inversely proportional to their average distance from the transducer, which enables calculation of the height of the surface-grafted brush. The SPR response of a solution of BSA in HBS (ionic strength 150 mM, pH 7.5) injected on three different surface layers (Figure 2B) is lowest for a KDP peptide brush, higher for a KSP peptide brush and highest for a reference layer formed by tri(ethylene glycol)-undecanethiol. Analyzing these signals using the procedure described in the Materials and Methods section, we obtained brush heights of 5.7 nm and 9.8 nm for the KSP and KDP brushes respectively (Figure 2C).
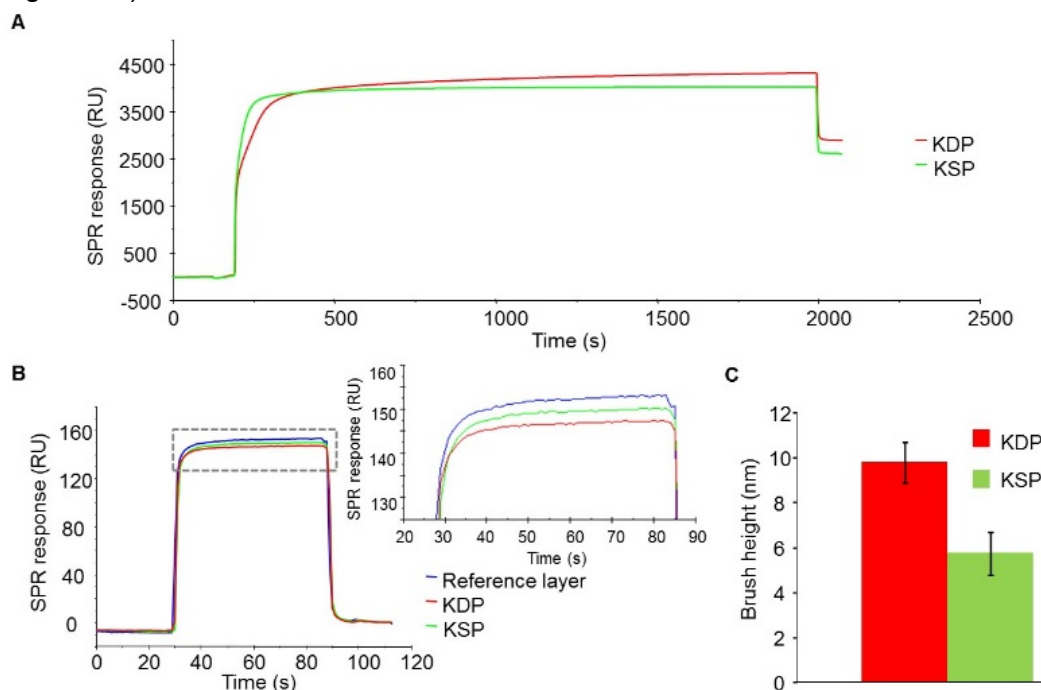

Figure 2. (A) Representative SPR responses for the immobilization of KSP and KDP peptides on SPR transducer surfaces. (B) Representative SPR responses during the injection of BSA dissolved at a concentration of 1 mg/ml in HBS (pH 7.5, ionic strength 150 mM) on surfaces functionalized with KSP and KDP brushes, as well as on a reference layer composed of tri(ethylene glycol)-undecanethiol. The inset shows an enlarged view of the indicated region. (C) Average heights of KSP and KDP brushes at pH 7.5 and ionic strength 150 mM obtained from three separate experiments. The error bars represent standard errors calculated from the three experiments. Each experiment included three injections of BSA.

We next tested the responsiveness of these peptide brushes to changes in pH. To do this we injected BSA in HBS of ionic strength 150 mM at different pH (pH 5 and 10), and analyzed the BSA signals following the procedure described above. This showed that the brushes underwent significant collapse at pH 5, shrinking to around half of their previous thickness (Figure 3A). This could be explained by the fact that the nominal charge on both peptides is lower at pH 5 than at pH 7.5 (Figure 1A). In contrast, both brushes experienced a modest expansion at pH 10, compared to at pH 7.5 (Figure 3A), which again correlates with the increase in the nominal charge on the peptides at pH 10 (Figure 1A). This is consistent with the behavior of a polyelectrolyte or polyampholyte brush, where the brush height depends strongly on chain charge. Furthermore, the extreme sensitivity of the brush height close to the nominal isoelectric point (pI) of the peptide, and comparatively lesser sensitivity at distant pH values is in agreement with our previous measurements with the full-length unphosphorylated NF-sidearm domain.[13] Subsequently, we studied the responsiveness of these brushes to changes in ambient ionic strength at pH 7.5. Again, taking the approach described earlier, we injected BSA in HBS at pH 7.5 of varying ionic strengths and analyzed the SPR signal. We observed significant adsorption of BSA at ionic strengths below 100 mM, possibly due to electrostatic attractive forces between BSA and the brushes, and so we confined our study to ionic strengths > 100 mM. In the ionic strength range of 100 mM-500 mM, the brushes demonstrated very interesting and distinct responses to ionic strength (Figure 3B). For the

KDP brushes, we observed a continuous decrease in brush height with increasing ionic strength. This behavior agrees with theories developed for polyampholyte and polyelectrolyte brushes, where increasing salt concentration enhances the screening of electrostatic repulsive forces between monomers and thus produces brush collapse.[18, 19] This also correlates with the trend in the R_g of KDP peptide, where increasing ionic strength causes a reduction in the average polymer coil size (Figure 1C). In contrast, the KSP peptide layer is relatively insensitive to ionic strength below 400 mM but undergoes significant expansion at 400 mM, followed by a collapse at 500 mM. While this unexpected behavior is not predicted by relevant mean field theories, the increase in height of the KSP brush at 400 mM can be hypothesized to be driven by similar mechanisms that cause the high-salt expansion of the KSP peptide at >200 mM in solution (Figure 1C).
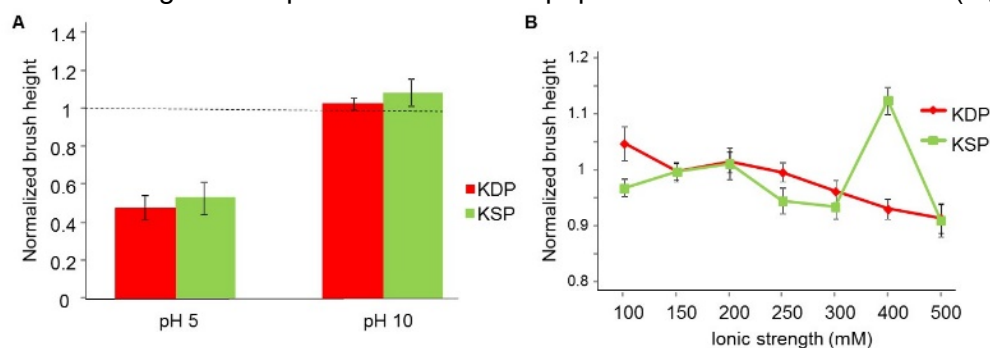

Figure 3. (A) Heights of KSP and KDP brushes at pH 5 and 10 and ionic strength 150 mM normalized to their individual heights at pH 7.5 and ionic strength 150 mM. (B) Heights of KSP and KDP brushes at pH 7.5 and varying ionic strengths normalized to their individual heights at pH 7.5 and ionic strength 150 mM. Three experiments, each consisting of three BSA injections, were conducted, and heights were normalized for each experiment independently. The data presented are the mean and standard error of the normalized heights obtained from the three experiments.

A possible criticism of this SPR-based technique for measuring brush height is that it can be affected by adsorption of BSA to the brushes. While we do not observe any significant adsorption of BSA onto peptide-functionalized surfaces in the ionic strengths presented here, we still cannot definitively rule out transient BSA adsorption. To verify these findings with a completely independent methodology, we measured the heights of the peptide brushes using scanning angle interference microscopy (SAIM).[20] SAIM measures the optical distance (product of physical distance and the refractive index of the intervening medium) of fluorescent species immobilized on special transducers composed of a thin film of silicon dioxide deposited on a reflective silicon wafer. The intensity of the fluorescence excitation light is axially modulated by varying the angle of incidence. Thus, the fluorescence intensity is a function of the incident angle of excitation light and the distance of the fluorophore from the silicon oxide layer (Figure S1 of ref[21]). This angle-dependent variation in intensity is then fit to a model (see Supporting Information of ref[21] for details) to extract the height of the fluorophore above the substrate. While SAIM has been applied with great success to measure intermolecular dimensions within cellular adhesion complexes, it has not as yet been applied to reconstituted polymer brushes. We therefore first verified the ability of SAIM to measure brush heights in a defined system in which thiol-terminated fluorescein-labeled PEG (molecular weight 5000 Da) was covalently immobilized to maleimide-functionalized SAIM substrates at high density. The curve for fluorescence intensity as a function of angle of incidence of excitation light for the PEG brush is shifted to the right of the curve for a comparable substrate that was functionalized with fluorescein (i.e. without the intervening PEG polymer), which confirms the higher thickness of the PEG brush (Figure S2A of ref[21]). Based on this observation, we extracted heights of 6 nm and 15 nm for fluorescein- and PEG-functionalized surfaces, respectively (Figure S2B of ref[21]). The height of the PEG layer could then be calculated as the difference between these two values (9 nm), which agrees with previously published heights of brushes made using PEG of this molecular weight and at comparable density.[17]

Having established SAIM as a suitable method to measure polymer brushes, we attempted to measure the heights of KSP and KDP peptide brushes using this technique. Towards this end, we first synthesized KSP and KDP peptides containing a cysteine on the C-terminus and labeled with fluorescein on the N-terminus. For SAIM studies, we used sequence-reversed retropeptides (PSK rather than KSP repeats; Figure S3A of ref[21]), which facilitated the use of the N-terminus for conjugation of fluorescein on resin, and allowed immobilization via the C-terminal cysteine, while still maintaining the original order of the sequence of amino acids relative to the substrate. We followed the immobilization of these retropeptides on quartz substrates functionalized with

maleimide groups using quartz crystal microbalance with dissipation monitoring (QCM-D) (Figure 4A). We calculated a nearest neighbour grafting distance of 2.2 nm between each polymer chain using a Voigt-Voinova model to fit the QCM-D data[22] and assuming a square packing of the peptides. While this distance was greater than the grafting distance achieved in the SPR experiments, it was approximately half of the end-to-end distance of the two peptides, ensuring that the immobilized peptides adopted brush conformations. We next measured the heights of the brushes in HBS (ionic strength 150 mM, pH 7.5) using SAIM (Figure 4B). In concurrence with the observations from the SPR-based measurements, we confirmed that the KSP peptide forms a thinner brush than KDP (3.7 nm and 5.0 nm for KSP and KDP respectively). The lower heights of the brushes in comparison to the SPR experiments can be explained by the lower surface density in the SAIM experiments. In addition to the different grafting densities, another possible reason for the discrepancy between the heights measured by the two techniques is that the data obtained from the SAIM measurements is modeled using a constant refractive index of the layer (1.33), which may not be strictly correct. In spite of these apparent differences in the absolute brush heights obtained from these two complementary techniques, the strong qualitative agreement between these two independent methodologies supports the notion that KDP peptides form thicker brushes than KSP peptides under comparable grafting densities and solution conditions.
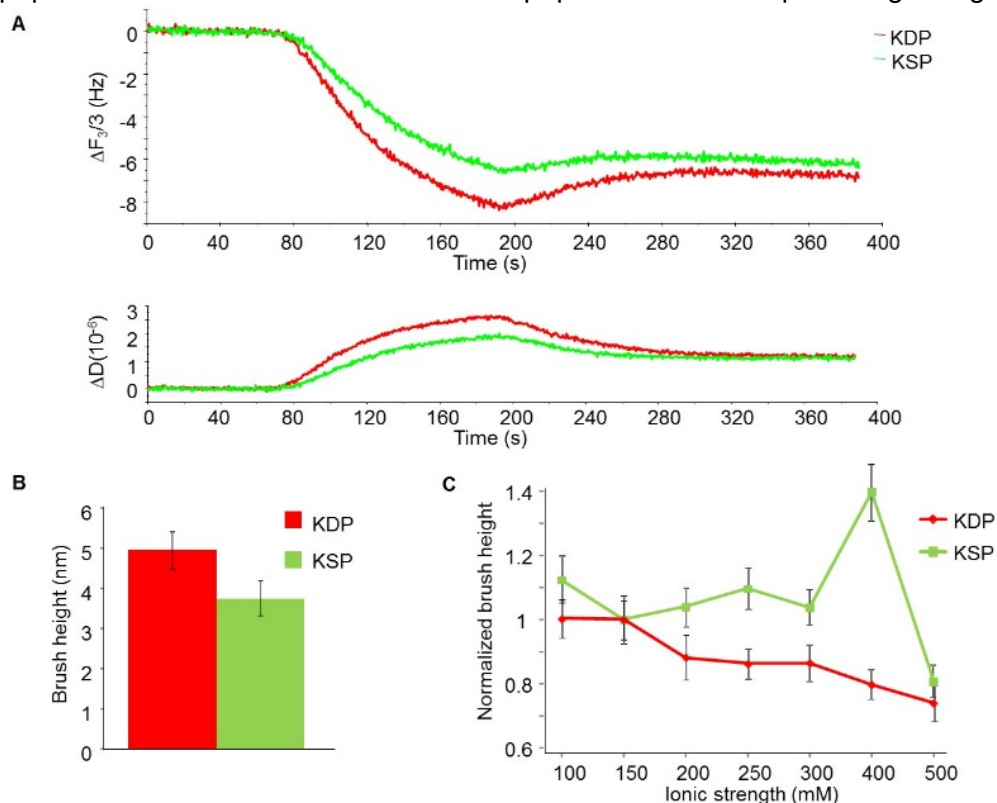

Figure 4. (A) Change in frequency and dissipation (first overtone) signals upon immobilization of KSP and KDP peptides on substrates functionalized with maleimide groups as detected using QCM-D. (C) Heights of KSP and KDP brushes at pH 7.5 and ionic strength 150 mM measured using SAIM. (C) Heights of KSP and KDP brushes measured using SAIM at pH 7.5 and varying ionic strengths normalized to their individual heights at pH 7.5 and ionic strength 150 mM. Three experiments were conducted, and heights were normalized for each experiment independently. The data presented here are the mean and standard error of the (normalized) heights obtained from the three experiments.

We next conducted SAIM measurements on the peptide brushes under varying ionic strengths. We again observed trends that closely follow the ones observed using the SPR experiments (Figure 4C). KDP peptide brushes displayed a monotonic decrease in brush height with ionic strength. The brush height of KSP peptides, on the other hand, was largely non-responsive to ionic strength to 400 mM followed by an abrupt increase at 400 mM, and a subsequent drop at 500 mM. Notably, the height of a surface that was functionalized only with fluorescein did not change with ionic strength (data not shown), confirming that the observed brush height variations reflect the dynamics of the peptide brushes rather than any ionic strength-dependent influences on the underlying surface chemistry or fluorescein fluorescence. As with the comparison between KSP and KDP

peptides in solution, these SAIM experiments confirm SPR findings that these two peptides display distinct dependences on ionic strength.

We published a paper based on this work in *Langmuir*.[21]

B. PROTEIN-BASED STRATEGY
As described above and in previous reports, we also pursued a strategy based on biosynthesis of recombinant intrinsically disordered proteins (IDPs).   Our IDP (termed rNFH-SA) was based on human NF-H and includes ~50 KSP-containing repeats, as well as an N-terminal tetracysteine sequence for chemical conjugation and a C-terminal His-tag for purification. In our 2014 report, we described our characterization of this protein by dynamic light scattering, which indicated that the protein adopts an extended conformation with a hydrodynamic radius of ~10 nm, much larger than the expected value for a folded protein. We also confirmed that rNFH-SA lacks secondary structure by circular dichroism spectroscopy, which revealed predominantly random coil secondary structure. We then demonstrated our ability to graft rNH-SA at high densities in an oriented fashion to solid supports, which we characterized with quartz crystal microbalance with dissipation (QCM-D). Finally, we showed that the resulting IDP brush swells and collapses under external stimuli, such as pH and ionic strength, as measured by atomic force microscopy (AFM), yielding nearly a six- to tenfold dynamic range in brush thickness as ionic strength is varied and a fourfold range as pH is varied.

An additional and relatively unique feature of a protein-based brush is the ability to incorporate proteolytic cleavage sites into the polymer chain, which should in principle enable shortening or "shaving" of the polymer brush with high precision upon addition of the cognate protease. To explore this concept, we assembled rNFH-SA brushes and applied one of two proteases: thrombin, a serine protease that cleaves rNFH-SA at a recognition site (LVPR|GS) located just ahead of the HN-tag on the C-terminus of the protein, and clostripain, an ArgC endoproteinase that cleaves at five sites along the length of the protein, the deepest of which is 253 residues from the top edge of the brush (Fig. 5A). A droplet of the protease was incubated with the rNFH-SA brush for a defined time before being washed off, and then the C-terminal HN-tag was visualized by immunofluorescence (Fig. 5B-C). Both enzymes are capable of cleaving off the HN-tag as evidenced by the loss of fluorescence in the region exposed to the protease; furthermore, enzymatic cleavage was reasonably well-confined within the droplet boundary, effectively patterning the brush height via confined proteolysis. By treating with the appropriate enzyme and measuring resulting changes in brush height by AFM, we found that we could specifically and spatially "shave" the brush at the expected sites along the sequence, thereby modulating brush height *in situ* and under physiological conditions (Fig. 5D-E). Specifically, addition of thrombin produced a loss of fluorescence (indicating successful enzymatic cleavage) without producing a significant change in brush height by AFM. Conversely, addition of clostripain produced the same loss of fluorescence while reducing brush height by 20%. Thus, brush height may be modulated *in situ* to precise and predictable values by taking advantage of proteolytic cleavage sites, which in principle could be designed into the sequence *a priori*.

We published a paper based on this work in the journal *Nature Communications* in 2014.[23] This publication has received coverage in both the scientific and popular press, including a two-star rating in *Faculty of 1000*.

C. ENGINEERING NEURONAL BEHAVIOR VIA CYTOSKELETAL NETWORKS
We have sought to understand how adult neural stem cells (NSCs) sense and respond to mechanical signals in their environment. We have shown that the lineage commitment and differentiation of NSCs is strongly sensitive to the elasticity of the extracellular matrix (ECM), such that NSCs are cultured on highly compliant ECMs in the presence of mixed differentiation cues predominantly differentiate into neurons, whereas those cultured on stiff ECMs under identical media conditions predominantly differentiate into astrocytes. We have also used retroviral gene delivery strategies to introduce constitutively active and dominant negative versions of key mechanotransductive enzymes (RhoA, Rac1, Cdc42) and shown that in some cases the activity of these enzymes can rescue or potentiate the ECM-derived stiffness cues. Our first major paper on this topic was published in *Stem Cells* in late 2011, which was a major factor in my being awarded the 2012 Stem Cells Young Investigator Award. We then had a followup paper accepted to *Integrative Biology* extending these ideas to human pluripotent stem cells (hPSCs), including embryonic and induced pluripotent stem cells. We had a third paper accepted to *Scientific Reports* in which we showed that neurons grown on compliant ECMs are fully competent to undergo neuronal maturation and subtype differentiation.

D. MULTISCALE MODELING OF CELLULAR MECHANICS

As described in previous reports, we have also sought to develop multiscale computational models that permit one to relate changes in IDP biochemistry to the structural and mechanical problems. We initially began by developing a new multiscale model of cell migration on ECMs of defined biophysical properties that integrates local activation of biochemical signals with adhesion and force generation at the cell-ECM interface. Our manuscript based on this work was published in *PLoS ONE* in March 2011.
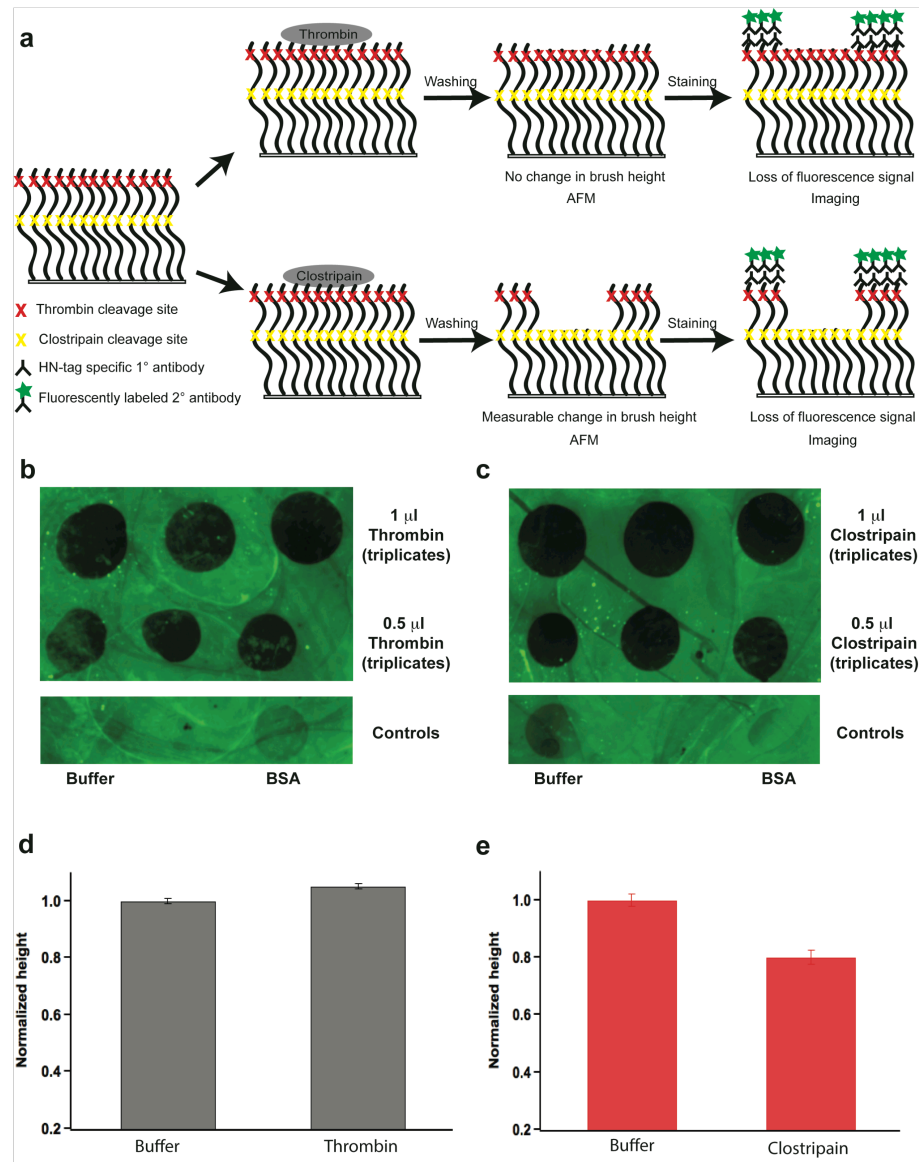

Figure 5. (A) Schematic representation of the protease digestion experiment (not to scale). Digestion is accomplished *in situ* on immobilized rNFH-SA brush. The thrombin cleavage site (x) is very close to the surface (19 amino acids deep) while the deepest clostripain digestion site (x) is 253 amino acids from the top edge of the brush. Although both enzymes cleave off the HN-tag leading to a loss of immunofluorescence, only clostripain digestion produces a measurable change in the brush height. Fluorescence image of the protein brushes digested with (B) thrombin and (C) clostripain. First row, 1 μl enzyme in triplicates; second row, 0.5 μl enzyme in triplicates; Third row, controls, left: buffer, right: BSA; The clostripain buffer contains Ca^{2+}, a divalent cation that could interact with the HN-tag;[1-3] these interactions likely affect the accessibility of the HN-tag to the antibody, thereby causing a minor decrease in fluorescence. Comparison of normalized brush heights calculated from AFM experiments for (D), thrombin and (E), clostripain digested surfaces. The brush heights were normalized to the height measured for the corresponding buffer incubated surface (57 ± 4 nm).

REFERENCES

1. Zheng, H., Chruszcz, M., Lasota, P., Lebioda, L. & Minor, W. Data mining of metal ion environments present in protein structures. *J Inorg Biochem* **102**, 1765-1776 (2008). 2872550
2. Harding, M.M. The architecture of metal coordination groups in proteins. *Acta Crystallogr D Biol Crystallogr* **60**, 849-859 (2004).
3. Ho, Y., Yang, M., Chen, L. & Yang, Y. Relative calcium-binding strengths of amino acids determined using the kinetic method. *Rapid Commun. Mass Spectrom.* **21**, 1083–1089 (2007).
4. Receveur-Brechot, V. & Durand, D. How random are intrinsically disordered proteins? A small angle scattering perspective. *Curr Protein Pept Sci* **13**, 55-75 (2012). 3394175
5. Petoukhov, M.V. & Svergun, D.I. Applications of small-angle X-ray scattering to biomacromolecular solutions. *Int J Biochem Cell Biol* **45**, 429-437 (2013).
6. Mertens, H.D. & Svergun, D.I. Structural characterization of proteins and complexes using small-angle X-ray solution scattering. *J Struct Biol* **172**, 128-141 (2010).
7. Bernado, P., Mylonas, E., Petoukhov, M.V., Blackledge, M. & Svergun, D.I. Structural characterization of flexible proteins using small-angle X-ray scattering. *Journal of the American Chemical Society* **129**, 5656-5664 (2007).
8. Bernado, P. & Svergun, D.I. Structural analysis of intrinsically disordered proteins by small-angle X-ray scattering. *Molecular BioSystems* **8**, 151-167 (2012).
9. Adiga, S.P. & Brenner, D.W. Molecular Basis for Neurofilament Heavy Chain Side Arm Structure Modulation by Phosphorylation. *Journal of Physical Chemistry C* **114**, 5410-5416 (2010).
10. Higgs, P.G. & Joanny, J.F. Theory of polyampholyte solutions. *The Journal of Chemical Physics* **94**, 1543-1554 (1991).
11. Müller-Späth, S., Soranno, A., Hirschfeld, V., Hofmann, H., Rüegger, S., Reymond, L., Nettels, D. & Schuler, B. Charge interactions can dominate the dimensions of intrinsically disordered proteins. *Proceedings of the National Academy of Sciences* **107**, 14609-14614 (2010).
12. Lee, J., Kim, S., Chang, R., Jayanthi, L. & Gebremichael, Y. Effects of molecular model, ionic strength, divalent ions, and hydrophobic interaction on human neurofilament conformation. *J Chem Phys* **138**, 015103 (2013).
13. Srinivasan, N., Bhagawati, M., Ananthanarayanan, B. & Kumar, S. Stimuli-sensitive intrinsically disordered protein brushes. *Nat Commun* **5**, 5145 (2014).
14. Kowalczyk, S.W., Kapinos, L., Blosser, T.R., Magalhães, T., van Nies, P., Lim, Y.H.R. & Dekker, C. Single-molecule transport across an individual biomimetic nuclear pore complex. *Nature Nanotech.* **6**, 433 - 438 (2011).
15. Deek, J., Chung, P.J., Kayser, J., Bausch, A.R. & Safinya, C.R. Neurofilament sidearms modulate parallel and crossed-filament orientations inducing nematic to isotropic and re-entrant birefringent hydrogels. *Nat Commun* **4** (2013).
16. Schoch, R.L., Kapinos, L.E. & Lim, R.Y. Nuclear transport receptor binding avidity triggers a self-healing collapse transition in FG-nucleoporin molecular brushes. *Proc Natl Acad Sci U S A* **109**, 16911-16916 (2012). 3479521
17. Schoch, R.L. & Lim, R.Y.H. Non-Interacting Molecules as Innate Structural Probes in Surface Plasmon Resonance. *Langmuir* **29**, 4068-4076 (2013).
18. Zhulina, E.B., Birshtein, T.M. & Borisov, O.V. Theory of Ionizable Polymer Brushes. *Macromolecules* **28**, 1491-1499 (1995).
19. Israels, R., Leermakers, F.A.M. & Fleer, G.J. On the Theory of Grafted Weak Polyacids. *Macromolecules* **27**, 3087-3093 (1994).
20. (!!! INVALID CITATION !!! 17, 18).
21. Bhagawati, M., Rubashkin, M.G., Lee, J.P., Ananthanarayanan, B., Weaver, V.M. & Kumar, S. Site-Specific Modulation of Charge Controls the Structure and Stimulus Responsiveness of Intrinsically Disordered Peptide Brushes. *Langmuir* (2016).
22. Voinova, M.V., Rodahl, M., Jonson, M. & Kasemo, B. Viscoelastic Acoustic Response of Layered Polymer Films at Fluid-Solid Interfaces: Continuum Mechanics Approach. *Physica Scripta* **59**, 391 (1999).
23. Srinivasan, N., Bhagawati, M., Ananthanarayanan, B. & Kumar, S. Stimuli-sensitive intrinsically disordered protein brushes. *Nature Communications* **5**, 5145 (2014).